International Journal of Biochemistry and Cell Biology 114 (2019) 105565

Contents lists available at ScienceDirect

International Journal of Biochemistry and Cell Biology

journal homepage: www.elsevier.com/locate/biocel

Trichostatin a inhibits phenotypic transition and induces apoptosis of the TAF-treated normal colonic epithelial cells through regulation of TGF-β pathway

Chao Huang[a,*], Xiao-fen Wu[b], Xiu-lian Wang[c]

[a] Department of Traditional Chinese Medicine, Affiliated Bao'an Hospital of Shenzhen, Southern Medical University, Shenzhen, 518100, China
[b] Department of Endocrinology, The 940th Hospital of Joint Logistics Support Force of Chinese People's Liberation Army, Lanzhou, 730050, China
[c] Health Management Centre, Affiliated Bao'an Hospital of Traditional Chinese Medicine of Shenzhen, Traditional Chinese Medicine University Of Guangzhou, Shenzhen, 518100, China

ARTICLE INFO

Keywords:
Histone deacetylase inhibitor
Tumor-associated fibroblasts
Epithelial-mesenchymal transition
Transforming growth factor-β
Colon

ABSTRACT

Tumor-associated fibroblasts (TAFs) contribute to transdifferentiation of stromal cells in tumor microenvironment. Epithelial-mesenchymal transition (EMT) is a procedure of phenotypic remodeling of epithelial cells and extensively exists in local tumoral stroma. Histone deacetylase (HDAC) inhibitor Tricostatin A (TSA) and sodium butyrate (SB) are reported to play important roles in the regulation of biological behaviour of cancer cells. However, whether TSA or SB is involved in control of EMT in colon epithelial cells induced by TAFs remains unidentified. In present study, we used conditioned medium (CM) form TAF-like CCD-18Co cells to stimulate 2D- and 3D-cultured colon epithelial HCoEpiC cells for 24 h and 4 d. We found that the CCD-18Co CM triggered multiple morphological changes in HCoEpiCs including prolonged cell diameters, down-regulation of E-cadherin and up-regulation of vimentin and α-SMA. Besides, ZEB1 and Snail expression and migration were also promoted by the CM. These phenomena were abolised by 5 μg/ml LY364947, a TGF-β receptor inhibitor. CCD-18Co induced up-regulation of HDAC1 and HDAC2 in the 2D and 3D models, while no change of HDAC4 expression was found. Treatment of 2 μg/ml TSA reversed the CCD-18Co-induced morphological changes and migration of the HCoEpiCs, and suppressed the downregulation of E-cadherin and upregulation of vimentin, α-SMA, ZEB1 and Snail. However, the suppressive effect of 4 mg/ml SB on the EMT was not observed. TSA down-regulated the expressions of Smad2/3, p-Smad2/3 amd HDAC4. Besides, TSA promoted the apoptosis rate (36.84 ± 6.52%) comparing with the CCD-18Co-treated HCoEpiCs (3.52 ± 0.85%, $P < 0.05$), with promotion of Bax (0.5893 ± 0.0498 in 2D and 0.8867 ± 0.0916 in 3D) and reduction of Bcl-2 (0.0476 ± 0.0053 in 2D and 0.0294 ± 0.0075 in 3D). TSA stimulated expression of phosphorylated-p38 MAPK in 2D (0.3472 ± 0.0249) and 3D (0.3188 ± 0.0248). After pre-treatment with p38 MAPK inhibitor VX-702 (0.5 mg/ml), the apoptosis rate of TSA was decreased in 2D (10.32%) and 3D (5.26%). Our observations demonstrate that epigenetic treatment with HDAC inhibitor TSA may be a useful therapeutic tool for the reversion of TAF-induced EMT in colon epithelium through mediating canonical Smads pathway and non-canonical p38 MAPK signalling.

1. Introduction

There are abundant proofs about the processes of transdifferentiation that might happen between sromal cells, remolding the tumor microenvironment and changing the phenotypes of various cell types. The stromal niches of the tumor involve cells with multiple potential, which are part of a phenotypic continuum between the endothelial or epithelial and mesenchymal lineages (Rusu et al., 2018). In adition to the stromal cells, a great many cytokines and chemokines secreted by these cells and malignant cells are also contributed to the modifications of niche (Servais and Erez, 2013; Glentis et al., 2017), resulting in development and progress of cancer. As dominant members in stroma, cancer-associated fibroblasts (CAFs) or tumor-associated fibroblasts (TAFs) or myofibroblasts have a striking influence on the several biological behaviour of malignant cells through production of transforming growth factor-β (TGF-β) (Wang et al., 2019), a key inducer of differentiation.

On the other hand, communication with other stromal components

* Corresponding author.
E-mail addresses: huangchao06@163.com, huangchao3@mail.sysu.edu.cn (C. Huang).

https://doi.org/10.1016/j.biocel.2019.105565
Received 16 April 2019; Received in revised form 24 June 2019; Accepted 3 July 2019
Available online 03 July 2019

including epithelial cells is another characteristic of TAFs or CAFs (Mukaida and Sasaki, 2016). Increasing results have indicated that CAFs or TAFs can induce the occurrence of epithelial-mesenchymal transition (EMT) (Goulet et al., 2019; Zhu et al., 2019). In the process of CAF-induced EMT, TGF-β signalling plays crucial functions in mediation of EMT-associated transcription factors including twist1, snail and ZEB1 (Wang et al., 2018a; Lamouille et al., 2014). In this context, mediating TGF-β pathway triggered by TAFs/CAFs maybe an feasible strategy to prevent the transdifferentiation of epithelial cells into mesenchymal counterparts.

Post-translational modifications of histones play an important role in transcriptional regulation (Nakamura et al., 2018; Hatakeyama et al., 2018). Acetylation and deacetylation of histone tails, respectively mediated by histone acetyltransferase (HAT) and histone deacetylase (HDAC), regulate gene activation and repression (Kelly et al., 2018; Rodríguez-Blanco et al., 2019). Cumulative evidence suggests aberrant HAT and HDAC activities in several cancer cells (Yu et al., 2018; Shanmugam et al., 2017). Interestingly, several HDAC inhibitors, including tricostatin A (TSA), sodium butyrate (SB), and polyoxometalate (POM), now are promising anticancer and anti-fibrosis agents in colon cancer owing to their involvement in transcriptional regulation of specific cancer-related genes(Sanaei et al., 2018; Al Emam et al., 2018; Lee et al., 2018; Bijelic et al., 2019) or signalling pathways involving in cell growth and differentiation, apoptosis, anti-inflammation, cell cycle (Fig. 1) (Li et al., 1996; Hassig et al., 1997; Bordonaro et al., 1999; Yin et al., 2001; Bordonaro et al., 2002; Klampfer et al., 2004; Ulrich et al., 2005; Archer et al., 2005; Calonghi et al., 2006; Stempelj et al., 2007; Kim et al., 2007; Nawrocki et al., 2007; Lecona et al., 2008; Backlund et al., 2008; Chowdhury et al., 2009; Lobjois et al., 2009; Sikandar et al., 2010; Serpa et al., 2010; Hsu et al., 2012a; Tang et al., 2012; Barrasa et al., 2012; Li and Chen, 2012; Zhan et al., 2012; Rajendran et al., 2013; Shin et al., 2014; Ji et al., 2015; Bordonaro and Lazarova, 2015; Raynal et al., 2016; Lazarova and Bordonaro, 2016; Bordonaro and Lazarova, 2016; Dasgupta et al., 2017; Schäfer et al., 2017). These mediated signalling pathways are presented in Fig. 1. In 2009, TSA or sodium butyrate (SB) was found to regulate the EMT and induce apoptosis of colon cancer cells, and these effects were associated with TGF-β and p38 MAPK signalling regulation (Stempelj et al., 2007; Kim et al., 2007; Nawrocki et al., 2007; Lecona et al., 2008; Backlund et al., 2008; Chowdhury et al., 2009; Lobjois et al., 2009; Sikandar et al., 2010; Serpa et al., 2010; Hsu et al., 2012a; Tang et al., 2012; Barrasa et al., 2012; Li and Chen, 2012; Zhan et al., 2012; Rajendran et al., 2013; Shin et al., 2014; Ji et al., 2015; Bordonaro and Lazarova, 2015; Raynal et al., 2016; Lazarova and Bordonaro, 2016; Bordonaro and Lazarova, 2016; Dasgupta et al., 2017; Schäfer et al., 2017; Sundararajan et al., 2019). POM, an emerging class of inorganic metal oxides, demonstrates promising antiproliferative activity against human colon adenocarcinoma cells. Inhibition of HDACs by POMs results in the accumulation of acetylated histones, leading to fatal changes in the expression of genes. POM can induce apoptosis through enhancement of the expression of pro-apoptotic components (Bax and Bim) and the reduction of the expression of anti-apoptotic components (bcl-2 and NF-KB) (Bijelic et al., 2019). However, the targets of the above studies are colon cancer cell, whether similar mechanisms exist in the TAF-induced EMT of colon epithelial cells is still unknown. In this study, we observe that HDAC1/2 was over-expressed in the TAF-induced EMT, while HDAC4 expression was not changed, TSA but not SB treatment significantly inhibited the EMT through regulation of TGF-β/Smads signalling and induced apoptosis through stimulation of p38 MAPK. These are reported below.

2. Materials and methods

2.1. Cell line origin and culture

The HCoEpiC, a human normal colon epithelial cell line from American Type Culture Collection (ATCC), was purchased GuangZhou Jennio Biotech Co., Ltd (China). CCD-18Co cells, a human colon myofibroblast line, were obtained from ATCC. Culture and maintenance of the two lines were performed as previous described (Yang et al., 2018).

2.2. Establishment of CCD-18Co cell-derived conditioned media (CM) and induction of HCoEpiCs

Procedure of preparation of CCD-18Co-derived CM cells was performed according to the literature (Wang et al., 2018b). In brief, The CCD-18Co cells were cultured with serum-free medium for 48 h, and collected the cell supernatants (conditioned medium, CM). Then centrifugation by 1650 *g* for 3 min was made. The HCoEpiCs cultured with free-serum media were further treated by 25% CM or the CM containing LY364947 or TSA or SB for 24 h, respectively. In 3D-cultured HCoEpiC cells, after multicellular spheroids were formed, the medium was replaced by CM (serum-free), continuing culture for 4 d. Phase contrast microscope was used to observe the morphological changes of HCoEpiCs (the same below).

2.3. Establishment of 3D culture model

The 3D culture of HCoEpiC cells was performed by relative literature (Koledova, 2017). Briefly, thawed Cultrex® Basement Membrane

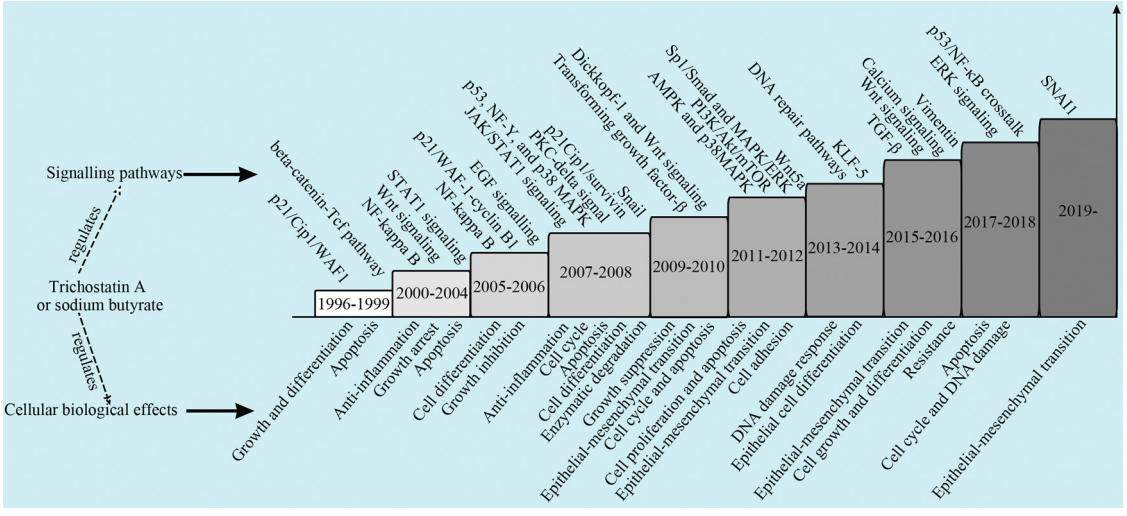

Fig. 1. The chronology of the major events in the field of HDAC inhibitor tricostatin A (TSA) or sodium butyrate (SB) and colon cancer.

Extract (BME) (overnight at 4 °C) was mixed by slowly pipetting solution up and down. Pipetting 200–300 μl per cm^2 BME onto each well of a twelve-well culture plate at 37 °C for 30 min. After a solidification was formed., the BME was overlaid with 400 μl of complete medium containing 1×10^4 trypsinized cells and 3% Cultrex® BME. The medium was updated every 2–3 days. Imaging of 3D morphology was collected.

3. Immunofluorescence (IF) staining for E-cadherin

Normal HCoEpiC cells (1×10^4/well) in 2D and HCoEpiC cells treated by CM or LY364947 or TSA/SB for 4 d in 3D were performed by trypsinization and plated on 15-mm coverslips pre-placed into 6-well plates, and incubated for 24 h. The normal HCoEpiC cells were treated with CM or LY364947 or TSA/SB for 24 h. All the coverslips were washed three times with PBS (pH 7.4), fixed with 4% paraformaldehyde, and incubated for 30 min in blocking solution (10% sheep serum). The coverslips were incubated with anti-E-cadherin (1:200) primary antibodies at 4℃ overnight, followed by incubation of goat anti-mouse AlexaFluor-488 antibodies (E-cadherin) for 2 h at 37℃. The cell nuclei was counterstained with 4′,6-diamidino-2-phenylindole (DAPI) (C1005, Beyotime, China) for 3 min at room temperature. Morphology of the cells was observed using a fluorescence microscope (Olympus) equipped with a 960S-Fluor oil immersion lens. Mean fluorescence intensity of each picture was calculated by Image-Pro®Plusv6.0 (Media cybernetics, America).

3.1. Wound healing assay

An *in vitro* wound healing assay was used to observe the migration. A dish which coated with 90% confluenced HCoEpiC cells was wounded using a sterile 200-μl pipette tip in a " + " shape. Then the cells were treated by different conditions as mentioned above. Healing of wound was observed using the phase contrast microscope at 0 h, 6 h, 12 h, 18 h, and 24 h, respectively, and the degree of healing was quantified by an image analysis software Image J (National Institutes of Health, America).

3.2. Apoptosis of detection by flow cytometry

All detection procedure was performed by specification of Annexin V/Propidium Iodide (PI) kit. In brief, suspension cells (5×10^5) were collected and centrifuged (447.2 *g* for 5 min), followed by PBS washing for twice. Then, 500 μL binding buffer was added into the suspension, followed by 5 μL Annexin V, with 5 μL PI. Reaction was performed at room temperature for 10 min. The apoptosis rates were observed by flow cytometry (BD Biosciences AccuriC6, America).

3.3. Total RNA extraction and quantitative real-time polymerase chain reaction (qRT-PCR)

The cells treated by CM were washed and re-suspended in ice-cold TriZol solution (Invitrogen, USA), and then total mRNA was extracted by an RNA Easy Kit (Invitrogen), according to the manufacturer's instructions. The concentration of mRNA was measured by a micro-spectrophotometer K2800 (Kai'ao, Beijing, China), with the ratio of OD260/OD280 > 1.8. All reverse-transcription of total RNA into cDNA was performed using SYBR® Premix Ex Taq™ (Tli RNaseH Plus) and reverse Transcriptase M-MLV (RNase H-) (TAKARA, Japan). Performance of real-time PCR was realized by a CFX96 PCR system (Bio-Rad, USA), using the ViiA7 software (Thermo Fisher, USA), and the reaction system recommended by the manufacturer was used. Specific forward and reverse PCR primers were designed using a PRIMER5/NCBI system: E-cadherin: F: *GTACTTGTAATGACACATCTC*, R: *TGCCAGTTTCTGCATCTTGC*, 252 bp; Vimentin: F: *TCAGACAGGAT GTTGACAAT*, R: *GACATGCTGTTCCTGAATCT*, 404 bp; α-SMA: F: *GAAGCACAGAGCAAAAGAGG*, R: *CAGCAGTAGTAACGAAGGAATAG*, 445 bp; ZEB1: F: *GATGCGAAACGCGAGGTTTT*, R: *GCTTCTAGACAGG AAATCCCACA*, 72 bp; Snail: F: *CCAGTGCCTCGACCACTATG*, R: *GGG CTGCTGGAAGGTAAACT*, 119 bp. β-actin was served as an internal control in all reactions. The comparative cycle threshold (ΔCt) method was used to quantify normalized target gene expression relative to the internal β-actin. Data are shown as the relative gene expression $= 2^{-\Delta\Delta Ct}$.

3.4. Western blotting analysis

For performance of a western blotting, 10 μg of each protein sample was separated, electrotransferred, blocked in sequence. Then, the membranes coated with target proteins were incubated with the specific primary antibodies at 4 ℃ overnight, including E-cadherin, vimentin, α-SMA, ZEB1, Snail, Smad2, Smad3, p-Smad2, p-Smad3, Smad4, as well as HDAC1, HDAC2, HDAC4, p38 MAPK, Bcl-2, Bax, β-actin. Then incubation of horseradish peroxidase (HRP)-conjugated secondary antibodies was performed for 2 h at 37 ℃. All acquirement of protein bands and intensities was completed as previous shown (Yang et al., 2018).

3.5. Statistical analysis

All analysis of data were completed by a statistical software SPSS 20.0. The mean between multi-groups was compared using one-way ANOVA, and the LSD-*t* was used to perform post hoc multiple comparisons. Differences in statistics were significant ($P < 0.05$).

4. Results

4.1. TSA but not SB inhibits the CCD-18Co-induced EMT-like transition in 2D- and 2D-cultured colon HCoEpiCs

As the main cellular components, TAFs can secrete many stromal cytokines to trigger transdifferentiation of tumor cells or other stromal cells (Wawro et al., 2018). Among these cytokines, transforming growth factor-β (TGF-β) is one of the predominant members. Dedifferentiation of epithelial cells into TAFs/CAFs-like mesenchymal cells is likely a key origination of TAFs pool in tumor microenvironment (Aoto et al., 2018; Lakins et al., 2018). In such context, a positive feedback response may be existed between TAF/CAFs and epithelial cells. In present study, we firstly established preparation of CCD18-Co-derived conditioned medium (CM) to induce the colon epithelial cell HCoEpiCs, mimicking the crosstalk between TAFs and epithelial cells. As demonstrated in our previous study (Hassig et al., 1997), 25% CM triggered an *in vitro* EMT-like morphological transformation in 2D-cultured HCoEpiCs (Fig. 2A). Consistently, after 4 days of CM treatment, we seemingly observed some dispersive cells in the periphery of HCoEpiC organoids (Fig. 2B), comparing with the control. We speculate whether cell migration was occurred. To our knowledge, the cells undergoing EMT will reveal reinforced cell motility to promote migration (Papageorgis, 2015). E-cadhein is a biomaker of epithelial cells and its loss is the most significant characteristic of EMT. We performed a fluorescence detection for the marker. As shown in Fig. 2C–E, fluorescence and intensity of E-cadehrin expression of the CM-treated cells in 2D and 3D model were significantly lower that of the control (0.11845 ± 0.0158 vs 0.3584 ± 0.0189 in 2D; 0.1358 ± 0.0462 vs 0.4231 ± 0.0381 in 3D, $P < 0.05$). To verify these observations, we further performed a detection for the expression of epithelial and mesenchymal markers and EMT-associated transcription factors. Our detections found that CCD-18Co CM not only decreased the expression of E-cadherin, but also up-regulated the expressions of vimentin and α-SMA in these models. In addition, CM stimulated the expressions of ZEB1 and Snail (Figs. 3 and 4).

Considering the participation of TGF-β signalling in the EMT, a TGF-β receptor kinase I inhibitor LY364947 was added into the medium of

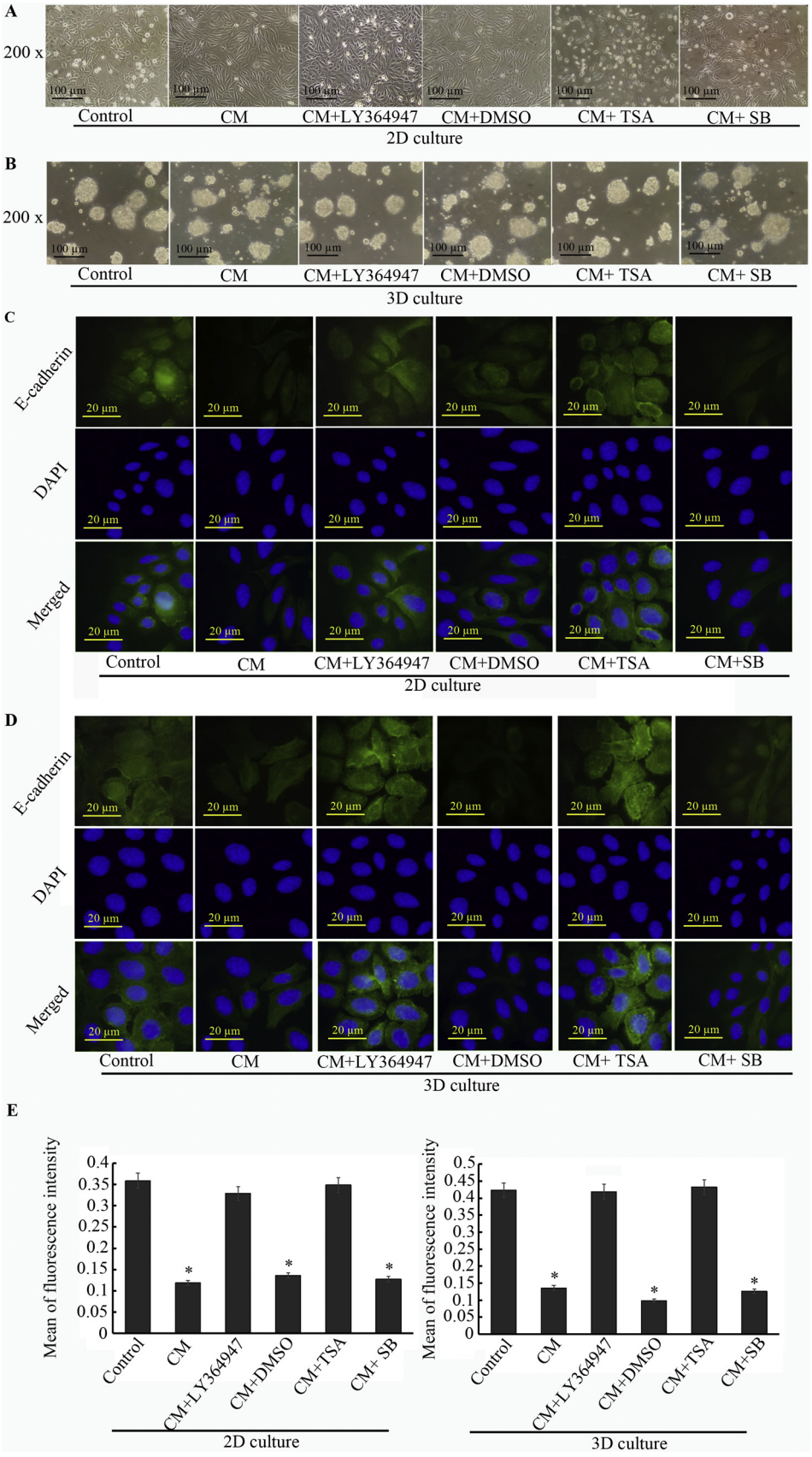

Fig. 2. Morphological observation of HCoEpiC cells in 2D and 3D culture by a phase contrast microscope (10 × 20) and cell immunofluorescence for E-cadherin (10 × 100). **A** HCoEpiCs in 2D culture are treated by 25% CCD-18Co-derived CM for 24 h, The cells in CM + LY364947 group and CM + DMSO group are treated by 5 μg/ml LY364947 or DMSO with 25% CM for 24 h. The CM + TSA or SB group is 2 μg/ml TSA and 4 mg/ml SB with 25% CM for 24 h. **B** In the 3D-cultured model, when the multicellular spheroids is formed, the 3D-cultured cells are treated by 25% CCD-18Co CM or LY364947, TSA and SB for 4 days. **C** Immunofluorescence of E-cadherin in 2D model. **D** Immunofluorescence of E-cadherin in 3D model. **E** Histogram of fluorescence intensity of E-cadherin. *$P < 0.05$ versus control.

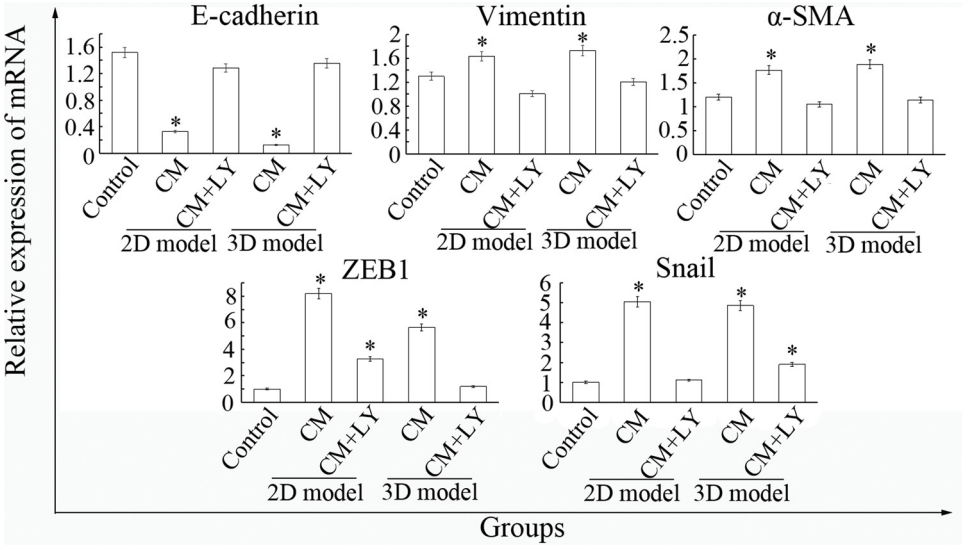

Fig. 3. Relative expression of mRNA for E-cadherin, vimentin, α-SMA, ZEB1 and Snail in the 2D and 3D models. These cells are treated CM or CM with LY364947 (LY). The error bar represents the SD (n = 3). *$P < 0.05$ versus control (ANOVA).

HCoEpiCs. As previous described, 5 μg/ml LY364947 repressed the CM-triggered EMT-like changes in HCoEpiCs (Fig. 2A-B), with E-cadherin up-regulation, and α-SMA and vimentin down-regulation (Fig. 2C–E and Fig. 3). These phenomena of LY364947 are similar to those of TSA but not SB. After treatment of CCD-18Co CM with 2 μg/ml TSA or 4 mg/ml SB for 24 h. We found that TSA but not SB also inhibited the EMT-like changes in 2D- and 3D-cultured HCoEpiCs (Fig. 2A-B). TSA obviously increased the fluorescence of E-cadherin comparing with the CM group (0.3489 ± 0.0865 vs 0.11845 ± 0.0158 in 2D; 0.4325 ± 0.0695 vs 0.1358 ± 0.0462 in 3D, $P < 0.05$), but this effect was not found in the SB-treated cells (Fig. 2C–E). These observations suggest that TSA but not SB takes part in the intervention of CCD-18Co-induced EMT in colon epithelial HCoEpiCs. With the help of western blotting, TSA increased the expression of E-cadherin and decreased the expression of α-SMA, vimentin, ZEB1 and Snail (Fig. 4A-B).

4.2. TSA suppresses the CCD-18Co-induced migration in HCoEpiC cells

Cell migration, a highly regulated biological process, are contributed to both physiological and pathological dysfunctions through promoting the cell mobility (Catalano et al., 2015). However, inhibition of EMT can prevent the occurrence and reinforcement of migration. It suggests that appearance of EMT is a crucial contributor and a potent prerequisite of cell migration. In present study, compared with the control, CCD-18Co CM significantly promoted the migration of HCoEpiCs at 6 h (1454 ± 126 × 10^3 *vs* 1074 ± 58 × 10^3 PPI), 12 h (1449 ± 73 × 10^3 *vs* 568 ± 26 × 10^3 PPI), 18 h (1446 ± 45 × 10^3 *vs* 550 ± 44 × 10^3 PPI) and 24 h (1417 ± 92 × 10^3 *vs* 346 ± 38 × 10^3 PPI) (Fig. 5A-B). Combining with the above results, our observations suggest that CCD-18Co CM-promoted migration may be in relation to the induction of EMT. Therefore, we hypothesized that inhibiting the EMT could abolish the CM-induced migration. The previous results revealed the suppression of TSA in the EMT. Consistently, 2 μg/ml TSA also repressed the CM-triggered migration in HCoEpiCs at 6 h, 12 h, 18 h, 24 h (Fig. 5A-B), comparing with the CM group (1415 ± 236 × 10^3 vs 1074 ± 58 × 10^3 PPI, 1421 ± 245 × 10^3 vs 568 ± 26 × 10^3 PPI, 1415 ± 106 × 10^3 vs 550 ± 44 × 10^3 PPI, 1242 ± 97 × 10^3 vs 346 ± 38 × 10^3 PPI, $P < 0.05$). These results indicate that the CCD-18Co cells induce the *in vitro* EMT-like changes in HCoEpiCs and TSA inhibits the migration. These phenomena may be associated with the suppression of mesenchymal genes and promotion of epithelial genes.

4.3. HDAC1 and HDAC2 involve the process of CCD-18Co-induced EMT in HCoEpiC cells and TSA regultes the components of TGF-β/Smad pathway

TGF-β signalling plays key functions during the EMT induction. As an activator of this signalling, TGF-β binds its receptors (TβRI and TβRII) to form a Smad2/3/4 complex. This complex is translocated into nucleus to mediate gene transcription associated with EMT (Wei et al., 2014; Lyu et al., 2018). In this scenario, regulation of Smads may be involved in the process of EMT induction. We found the increased expression of classical Smads including Smad2/p-Smad2 and Smad3/p-Smad3 in the 2D (0.5464 ± 0.0203/0.5383 ± 0.0614 and 0.6598 ± 0.1261/0.4275 ± 0.0325) and 3D (0.6564 ± 0.1124/0.3741 ± 0.0952 and 0.5328 ± 0.1132/0.5175 ± 0.1216) models (Fig. 6A-B). As common molecular partner of receptor-regulated Smads (RSmads), Smad4 in the nucleus and the RSmads (Smad2 and Smad3) can form a complex associated with additional DNA-binding cofactors. The complex promotes the high affinity and selectivity to specific target genes. As shown in our research, CCD-18Co CM induced the high expression of Smad4 in the 2D (0.4743 ± 0.0895 vs control 0.2544 ± 0.0926, $P < 0.05$) and 3D (0.4843 ± 0.1240 vs control 0.2744 ± 0.0897, $P < 0.05$) models (Fig. 6A-B). However, with the addition of LY364947, the above phenomena were inverted (Fig. 6). TSA decreased the expression of Smad2/p-Smad2 and Smad3/p-Smad3 in 2D (0.2674 ± 0.0546/0.4738 ± 0.1321 and 0.4316 ± 0.1021/0.2743 ± 0.0548) and 3D (0.4426 ± 0.1031/0.2689 ± 0.0503 and 0.2354 ± 0.0589/0.1982 ± 0.0298) models, comparing with the CM groups in 2D (0.2132 ± 0.0652/0.2002 ± 0.0135 and 0.1687 ± 0.0264/0.1954 ± 0.0342) and 3D (0.2368 ± 0.0548/0.2186 ± 0.0754 and 0.2485 ± 0.0845/0.3286 ± 0.0812) ($P < 0.05$).

Gene transcription is profoundly affected by the manner in which DNA is packaged (Wade, 2001). Histone deacetylase (HDAC) regulates the acetylation status of histones and thereby orchestrates the regulation of gene expression. In our study, HDAC1 and HDAC2 expressions were significantly up-regulated in the CCD-18Co CM-induced EMT-like changes of 2D- and 3D-cultured HCoEpiC cells (Fig. 6A-B). The expression level of HDAC1 and HDAC2 in 2D (0.8457 ± 0.0542 and 0.8757 ± 0.0749) and 3D (0.7657 ± 0.0462 and 0.6652 ± 0.0942) culture was respectively higher than that of control (0.1258 ± 0.0389 and 0.1588 ± 0.0843, 0.1058 ± 0.0563 and 0.1356 ± 0.0492) ($P < 0.05$). However, HDAC4 expression (0.2154 ± 0.0785 in 2D and 0.1457 ± 0.0465 in 3D) was not changed in the CM-treated cells,

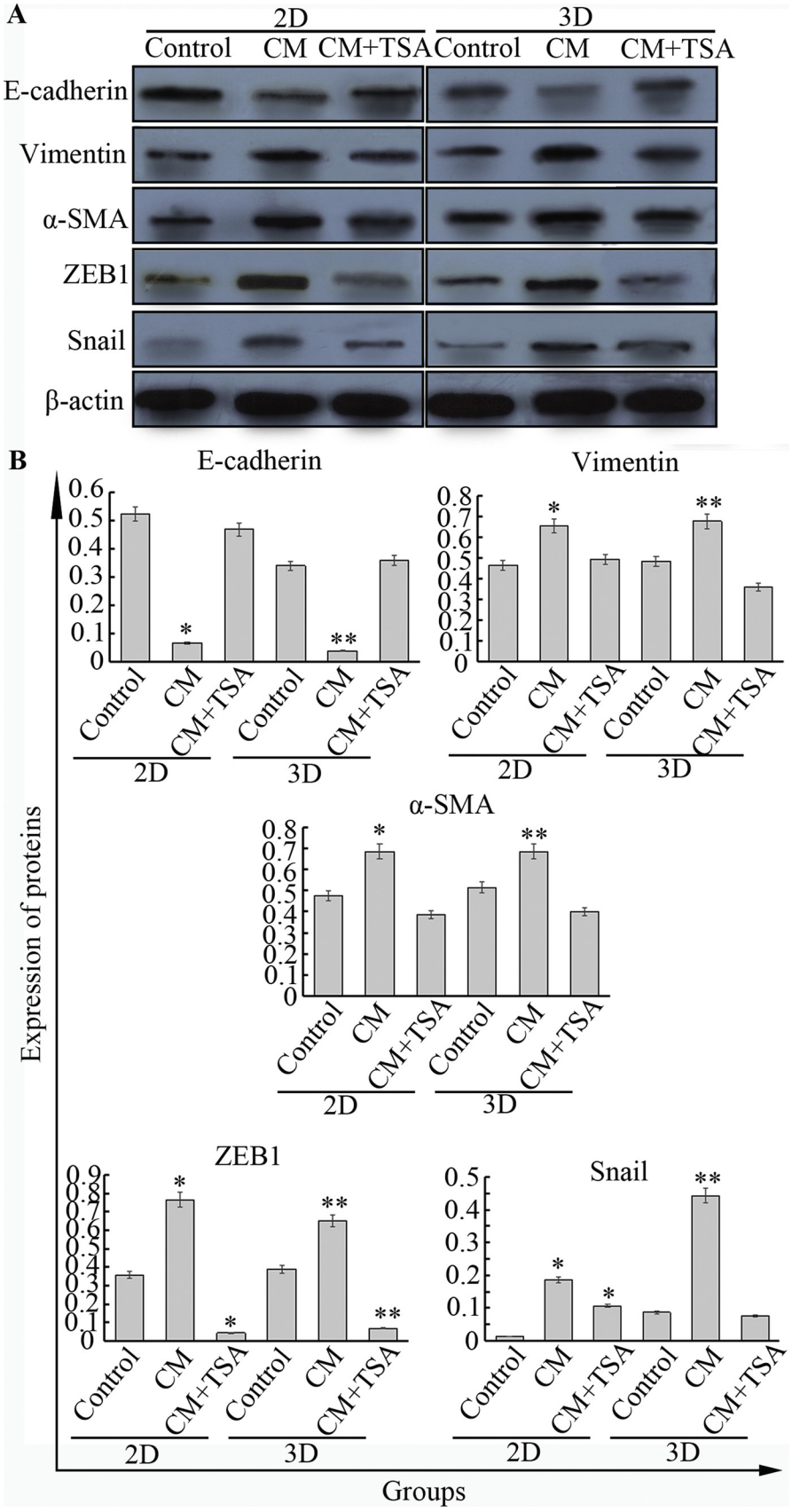

Fig. 4. Effect of TSA on EMT biomarkers and transcription factors in 2D- and 3D-cultured HCoEpiC cells. Control is the normal HCoEpiC cells without CM. **A** The effect of 2 μg/ml TSA on expressions of E-cadherin, vimentin, α-SMA, Snail and ZEB1 in the CM-treated HCoEpiCs, and these expressions was assessed by western blotting. **B** Histograms of expressions of E-cadherin, vimentin, α-SMA, Snail and ZEB1. The error bar represents the SD (n = 3). $^{*}P < 0.05$ versus control in 2D model, and $^{**}P < 0.05$ versus control in 3D model (ANOVA).

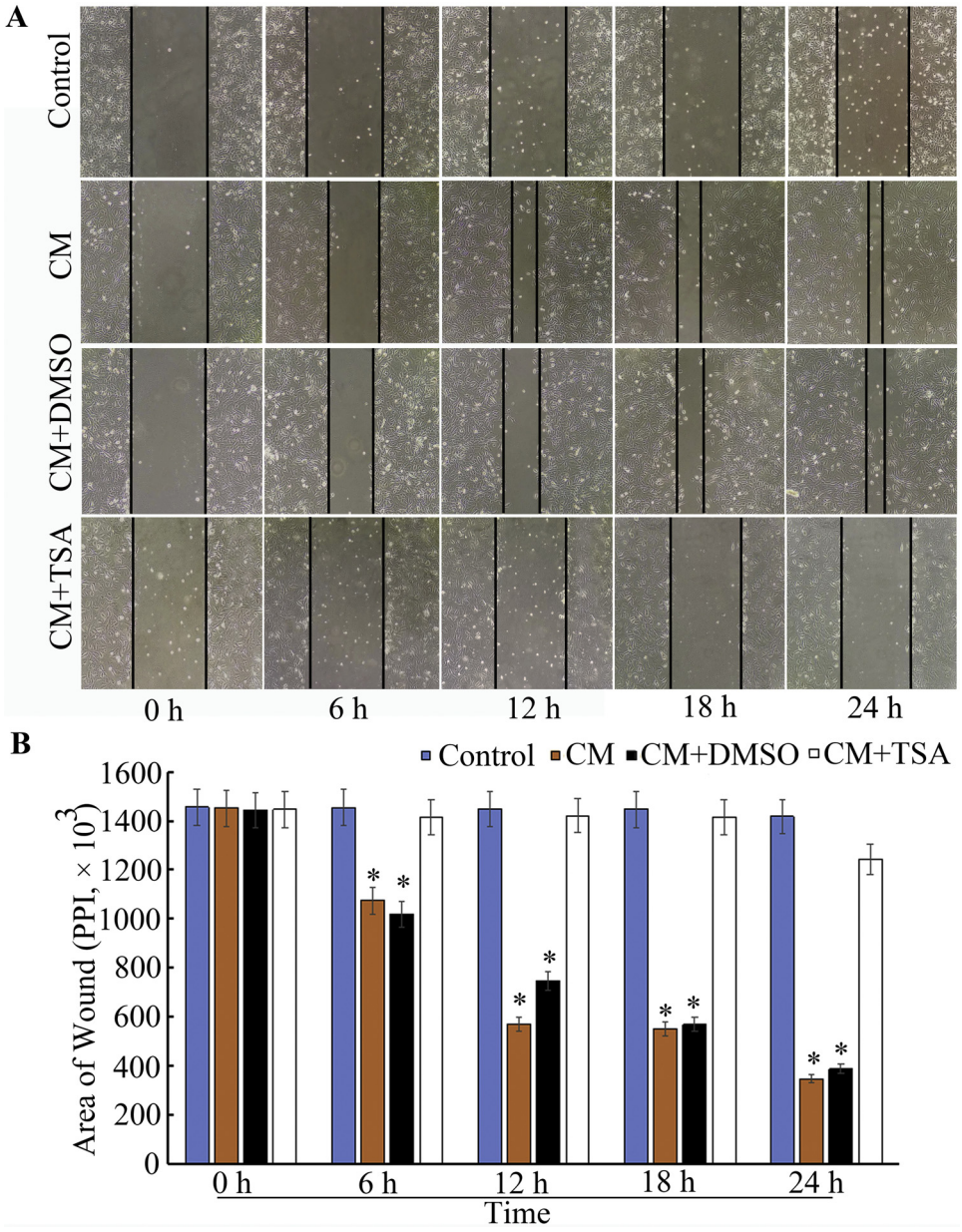

Fig. 5. Analysis of effect of 2 μg/ml TSA on HCoEpiC cells motility by wound-healing assay. **A** Area of wound in the HCoEpiC cells are observed by phase contrast microscopy (10 × 10). **B** Analysis of wound area by Image J, and the area of wound is presented by pixels per inch (PPI). The error bar represents the SD (n = 3). *$P < 0.05$ versus control (ANOVA).

comparing with the control in 2D (0.2288 ± 0.0286) and 3D (0.1257 ± 0.0746) ($P > 0.05$) (Fig. 6A-B). This suggests that inhibition of HDAC1/2 is likely to abolish the EMT process. A recent report has suggested that global suppression of HDAC activities by inhibitors inhibited TGF-β1-induced EMT in human renal proximal tubular epithelial cells (Yoshikawa et al., 2007a). TSA, a nonselective HDAC inhibitor, targets both class I including HDAC1/2 and class II HDACs including HDAC4. Several studies have shown that TSA suppressed proliferation and EMT of cancer cells and epithelial cells (Chen et al., 2013; Yoshikawa et al., 2007b). Unfortunately, it was not understood whether TSA can suppress the process of EMT induced by CCD-18Co in HCoEpiC cells. We observed that decreased expressions of HDAC1, HDAC2 and HDAC4 appeared in these cells treated with TSA in 2D (0.1633 ± 0.0478, 0.2945 ± 0.0758, 0.1345 ± 0.0654, respectively) and 3D (0.1145 ± 0.0412, 0.1497 ± 0.0798, 0.0644 ± 0.0326, respectively) models (Fig. 6A-B). Besides, TSA down-regulated the expressions of Smad2/p-Smad2 and Smad3/p-Smad3 in the 2D and 3D models, comparing to that of the cells treated with CM. However, we also observed that TSA increased the expression of Smad4 in the 2D and 3D models.

4.4. TSA induces apoptosis of HCoEpiC cells undergoing EMT triggered by CCD-18Co through up-regulation of phosphorylated-p38 MAPK

In addition to EMT suppression, TSA can also induce apoptosis in these EMT-like cells. Our observations revealed that 2 μg/ml TSA promoted the apoptosis rate in these 2D and 3D cells undergoing EMT, which was significantly higher than that in the cells with CM and DMSO (36.84 ± 6.52% *vs* 3.52 ± 0.85% and 3.68 ± 0.74%, $P < 0.05$, Fig. 7A). TSA also stimulated the expressions of pro-apoptotic Bax (0.5893 ± 0.0498 in 2D and 0.8867 ± 0.0916 in 3D) and suppressed the anti-apoptotic Bcl-2 (0.0476 ± 0.0053 in 2D and 0.0294 ± 0.0075 in 3D), comparing to the CM-treated cells in 2D (0.0546 ± 0.0128 of Bax and 0.2741 ± 0.0287 of Bcl-2) and 3D

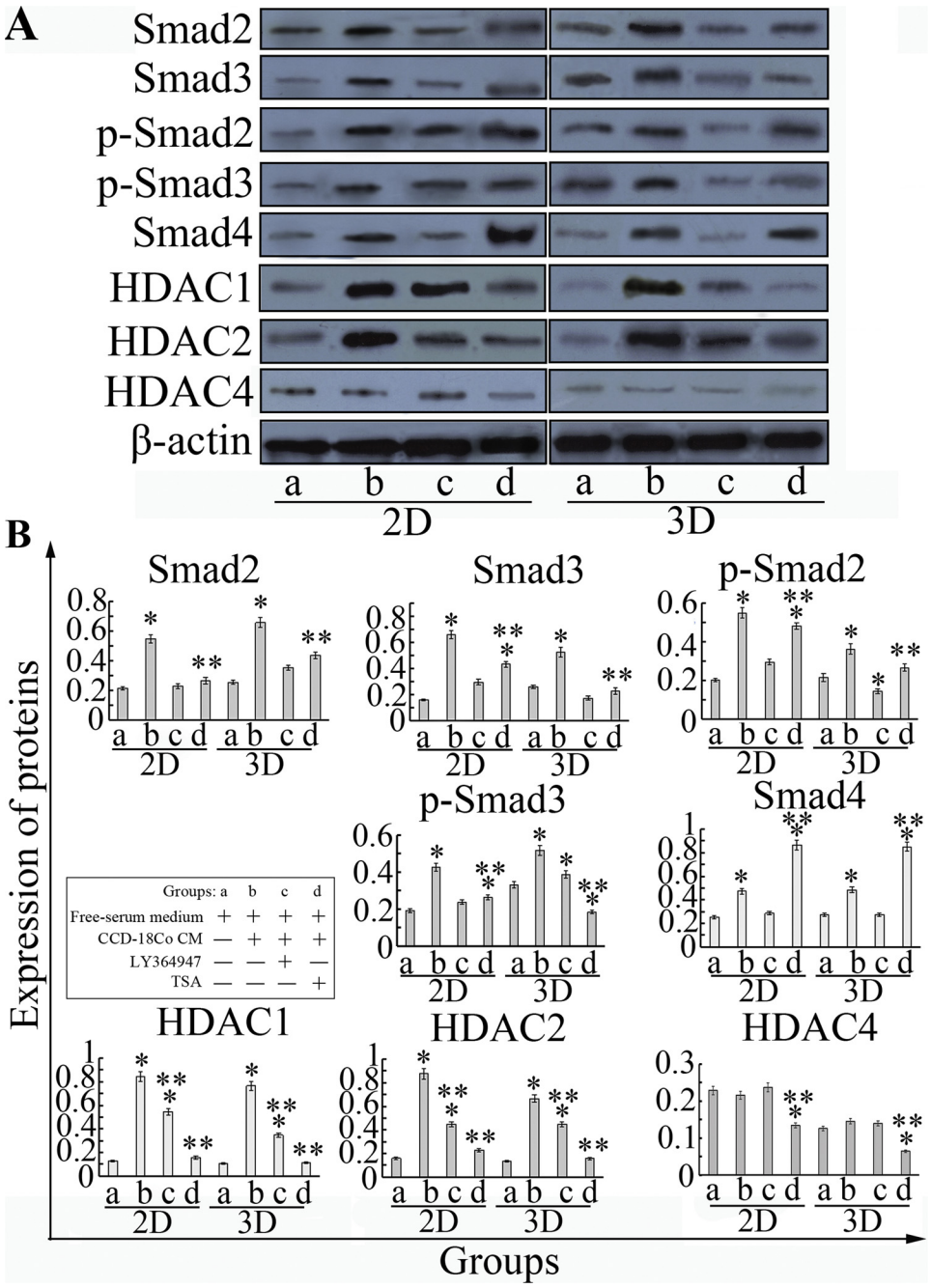

Fig. 6. Detection of HDAC1, HDAC2, HDAC4 and Smads by western blotting in 2D and 3D models. **A** Protein bands of western blot analysis in the cells treated by different conditions. **B** Analysis of expression for the protein bands. a: control, b: CCD-18Co CM, c: CCD-18Co CM + LY364947, d: CCD-18Co CM + 2 μg/ml TSA. The error bar represents the SD (n = 3). *$P < 0.05$ versus control, **$P < 0.05$ versus CM group (ANOVA).

(0.0551 ± 0.0107 of Bax and 0.3246 ± 0.0495 of Bcl-2) (Fig. 7B-C). Besides, TSA also promoted phosphorylated-p38 MAPK (p-p38 MAPK) expression in 2D (0.3472 ± 0.0249) and 3D (0.3188 ± 0.0248), which were higher than that of CM group in 2D (0.1257 ± 0.0463) and 3D (0.1842 ± 0.0625) ($P < 0.05$). However, pre-treatment of 0.5 mg/ml VX-702 (SD5960, Beyotime, China), an inhibitor of p38 MAPK, significantly decreased the TSA-induced apoptosis in 2D (10.32%) and 3D (5.26%) (Fig. 7A) and Bax expression in 2D (0.1356 ± 0.0842) and 3D (0.3864 ± 0.0285) comparing with the TSA group ($P < 0.05$) (Fig. 7B-C). These results suggest that p38 MAPK may be involved in the process of TSA-induced apoptosis.

5. Discussion

5.1. TAF-like CCD-18Co cells induce the EMT transformation of colon epithelial HCoEpiC cells through TGF-β signalling

Tumor-associated fibroblasts (TAFs), also named as myofibroblasts, play an important role during the remodeling of the surrounding matrix (Chen et al., 2018). TAFs can express several markers including vimentin, α-SMA, fibroblast activation protein (FAP) and platelet-derived growth factor receptors-β (PDGFR-β). Similar to the functions of TAFs, human colon CCD-18Co myofibroblasts (Giménez-Bastida et al., 2015, 2018) can also remodel the ECM (Pereira et al., 2015). In our study, we firstly demonstrated that CCD-18Co revealed significant fluorescence of

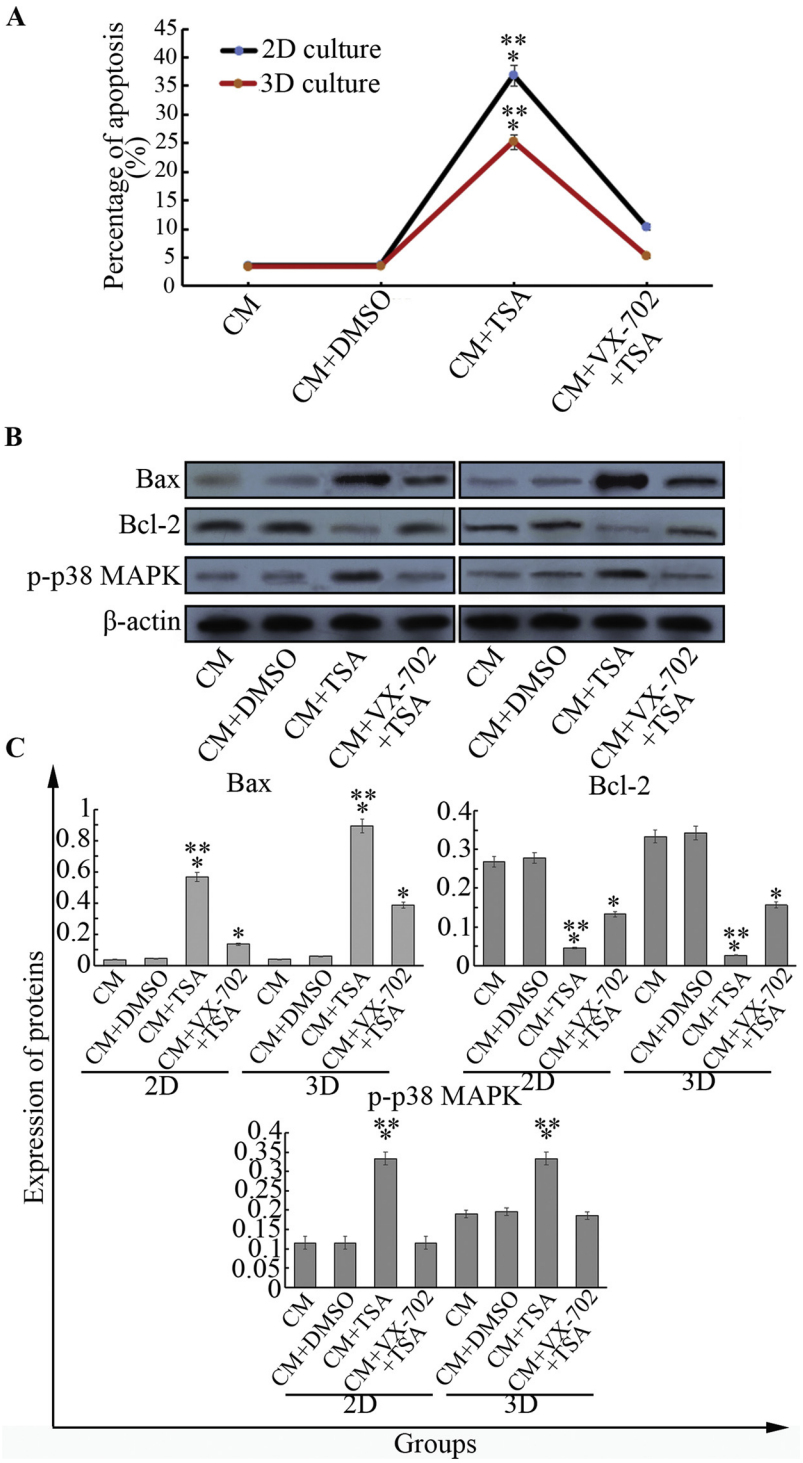

Fig. 7. Detection of cell apoptosis by flow cytometry and apoptotosis-assciated proteins and p38 MAPK in 2D and 3D models. **A** Percentage of cell apoptosis are acquired by Annexin V/Propidium Iodide (PI) kit through using flow cytometry and compared with CM group. The HCoEpiCs are treated with CM, CM + 2 μg/ml TSA and CM + 2 μg/ml TSA + 0.5 mg/ml p38 MAPK inhibitor VX-702 or without CM. **B** Bands of Bax, Bcl-2 and p38 MAPK in the TSA- or VX-702-treated cells are tested by western blotting. **C** Expression levels of the Bax, Bcl-2 and p38 MAPK. *$P < 0.05$ versus CM group, and ** $P < 0.05$ versus VX-702 (+) group (ANOVA).

vimentin, α-SMA, FAP and PDGFR-β, comparing with fluorescence expression of E-cadherin (view supplementary materials). Therefore, we selected the CCD-18Co as our TAF model. Loss of E-cadherin has been shown to be crucial in cancer development and EMT. Our results have shown that the CCD-18Co-derived conditioned medium (CM) induced the EMT-like changes in the 2D- or 3D-cultured colon epithelial cells HCoEpiCs, including spindle-like morphological changes, reduction of E-cadherin fluorescence and its protein expression, and enhancement of mesenchymal marker vimentin and α-SMA expression, with high expressions of Snail and ZEB1, as well as promotion of migration. In addition, these phenomena were abolished by a TGF-β receptor kinase I inhibitor LY364947, indicating that TGF-β signalling may be involved in the process of the CCD-18Co-induced EMT-like transition in HCoEpiCs.

5.2. HDAC1 and 2 involve in the process of the CCD-18Co-induced EMT of HCoEpiC cells

As a matter of fact, EMT is a reversible biological process, and epigenetic mechanisms extensively participate in this process (Sun and Fang, 2016; Musavi Shenas et al., 2018). Several studies have shown that large-scale epigenetic changes existed in EMT, and histone modification, one of the epigenetic modifiations, is crucial in the orchestration of EMT (Mobley and Abell, 2017).

Histone deacetylases (HDACs)-orchestrated epigenetic mechanisms play crucial functions in regulation of various physiological and pathological events (Tang et al., 2013). For example, up-regulation of class I and II HDACs was observed in TGF-β2 /TGF-β1-stimulated retinal pigment epithelium cells (Xiao et al., 2014), and cancer cells (Zhang et al., 2018; Orenay-Boyacioglu et al., 2018). Evidence from an *in vivo* study demonstrated that HDACs and Snail were essential for silencing E-cadherin in the metastatic process of pancreatic cancer cells (von Burstin et al., 2009). Inactivation or silence of E-cadherin in pancreatic cells can induce EMT, which is regulated by a transcriptional repressor complex containing Snail and HDAC1 and HDAC2. Our results revealed that the CCD-18Co CM increased the expressions of HDAC1 and HDAC2 but not HDAC4 in the 2D and 3D models, with up-regulation of Smad2/3, p-Smad2/3 and Smad4. These findings suggest that the expression of HDAC1 and HDAC2 may be associated with the TGF-β/Smads pathway. HDAC inhibitors are promising anticancer agents whose effects are correlated with the transcriptional regulation of specific cancer-related genes.

Recent evidence has shown that HDAC1, HDAC2 and HDAC6 are required for TGF-β1-induced EMT (Choi et al., 2016; Xu et al., 2017), which is consistent with our observations that no change of HDAC4 expression is found in the CM-treated cells. It suggests that HDAC4 may be not affected by the CM. HDAC1 is requisite for TGF-β1-induced EMT and cell migration in hepatocytes. It represses transcription of ZO-1 and E-cadherin involving in TGF-β1-induced EMT (Lei et al., 2010). Inhibition or silencing of HDAC2 can enhance the TGF-β1-induced EMT in A549 cells (Liu et al., 2018; Park et al., 2016a). Besides, global repression of HDAC activities by inhibitors, which are targets of both class I and class II HDACs, can inhibit TGF-β1-induced EMT in human renal proximal tubular epithelial cells (Yoshikawa et al., 2007c).

5.3. TSA but not SB inhibits the CCD-18Co-induced EMT and migration by suppression of HDAC1/2/4

TSA, a class I and II HDAC inhibitor, is demonstrated to modulate cell proliferation, differentiation, survival, apoptosis, cell migration and EMT (Adcock, 2007; Nagarajan et al., 2017). For example, TSA suppressed proliferation by G1 phase cell cycle arrest through inhibition of cyclin/CDK/p-Rb and induction of p21 and p27, and also prevented TGF-β2/TGF-β1-triggered EMT in retinal pigment epithelium cells through down-regulation of α-SMA, collagen type I, collagen type IV, fibronectin, Snail and Slug (Xiao et al., 2014). TSA inhibited TGF-β2-induced lens EMT (Xie et al., 2014), and decreased mRNAs and protein expressions of ECM components and prevented TGF-β1-induced EMT in normal rat kidney tubular epithelial cells (Noh et al., 2009). Thus, TSA suppressed EMT induced by TGF-β1 in human renal epithelial cells (Yoshikawa et al., 2007b).

HDAC1 and 2, class I HDACs, and HDAC4, class II HDAC, can be suppressed by TSA. Consistent with the previous results, our observations revealed that 2 μg/ml TSA inhibited HDAC1, HDAC2 and HDAC4 expression, and suppressed the CCD-18Co-induced EMT-like changes and migration in the HCoEpiCs, as well as up-regulated the expression of E-cadherin and down-regulated the expressions of vimentin, α-SMA, ZEB1 and Snail in the 2D and 3D models. Consistent with the results of previous study by Park (Park et al., 2016b), inhibition and silencing of HDAC2 and HDAC4 by TSA and siRNA enhanced TGF-β1-induced EMT in primary nasal epithelial cells A549, and TSA abolished the effect of TGF-β1 on the migratory ability of A549 cells. These data reveal that TGF-β1-induced EMT in airway epithelial cells via activation of HDAC2 and HDAC4, and that inhibition of HDAC2 and HDAC4 by TSA reduces TGF-β1-induced EMT. In our study, no influence of CM on HDAC4 expression is found, considering that HDAC4 expression is cell type dependent.

Sodium butyrate (SB), a histone deacetylase inhibitor for HDAC1, 2 and 7, respectively, can induce apoptosis, differentiation and promote the maturation of a variety of malignant cells, but SB shows no inhibition of HDAC6 and 10. Although SB is reported that it can induce changes in expression of EMT-related genes and proteins in cancer cells (Wang et al., 2013a; Mrkvicova et al., 2019), no effect of SB on the morphology of the CCD-18Co-stimulated HCoEpiCs is observed in our study. We think that the anti-EMT effect of SB may be cellular types dependent.

5.4. Smad2 and Smad3 but not Smad4 may be targets of TSA

Existing substantial evidence has demonstrated that classical TGF-β/Smad signalling pathway is associated closely with the proliferation, differentiation and migration (Siemens et al., 2011). Recent researches have validated that high activities of TGF-β-Smad2 signalling was participated in the establishment maintenance of EMT through epigenetic silencing of epithelial marker genes including E-cadherin (Dong et al., 2018). In our study, TSA down-regulated the expressions of Smad2/p-Smad2 and Smad3/p-Smad3 in the 2D and 3D models, comparing with the CM group. It reveals that Smads may be the targets for TSA against TAF-induced EMT. Although the function of Smad4 in colorectal cancer is not entirely clear so far, positive correlation of Smad4 with EMT transcription factors Snail-1, Slug and Twist-1 expression was found in colon tumor specimens (Ioannou et al., 2018). Our observation found that the expression of Smad4 was not be inhibited by TSA, demonstrating that Smad4 may be not affected by TSA. These data suggest that TSA inhibits CCD-18Co-triggered EMT in the HCoEpiCs through regulating TGF-β/Smad2/3 pathway.

5.5. TSA induces apoptosis of CCD-18Co-treated HCoEpiCs by mediating apoptotic protein Bax and Bcl-2 through activation of p38 MAPK pathway

TSA influence not only the canonical TGF-β/Smad pathway but also the non-canonical pathways including TGF-β/Akt, MAPK and ERK1/2 (Xiao et al., 2014). Thus, HDAC inhibitors can significantly suppress the growth of hepatocellular carcinoma cells, induce cell cycle arrest and apoptosis (Wang et al., 2013b). Substantial evidence has shown that non-Smad signallings are also participated in TGF-β-induced EMT in different types of cells, including PI3 K/Akt, p38 mitogen-activated protein kinase (p38 MAPK) and ERK1/2 pathways (Yao et al., 2008; Chen et al., 2012). Previous study has revealed that increased p38 MAPK expression existed during the TGF-β-induced EMT *in vitro*, which could be inhibited by enterolactone, leading to reversion of EMT (Mali et al., 2018). Consistent with the previous results, our study reveals that CM up-regulated the expression of p-p38 MAPK comparing with the control (0.0148 ± 0.0075, $P < 0.05$, data not shown in figures), suggesting that mediation of the p38 MAPK signalling plays an important role in inhibition of EMT (Chen et al., 2019).

However, p38 MAPK can also positively regulate occurence of cell death events including apoptosis. TSA can enhance the expression of histone H3 acetylation and MAPK phosphatase-1 (MKP-1) expression in IR lung tissue (Hsu et al., 2015). TSA also activates the phosphorylation of p38 MAPK, and inhibition of p38 MAPK signalling can in turn abrogate its effects of decreasing cell viability (Hsu et al., 2012b). In CCD-18Co-induced HCoEpiC cells, TSA dramatically promoted apoptosis of these cells, and increased pro-apoptotic protein Bax expression and suppressed anti-apoptotic protein Bcl-2 expression. Our results shown that TSA also induced the over-expression of phosphorylated-p38 MAPK (p-p38 MAPK). Therefore, we hypothesized that p38 MAPK was

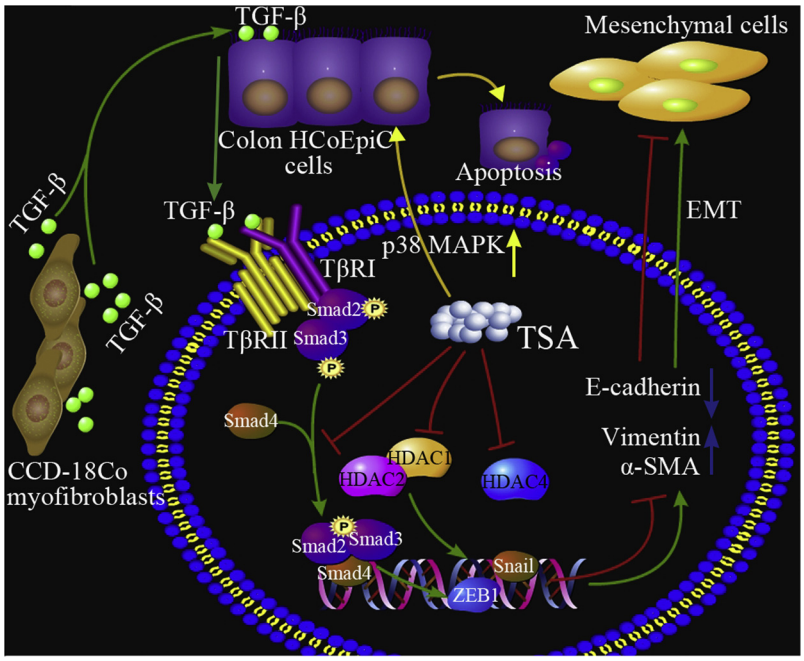

Fig. 8. The graphical abstract and highlights in present study. CCD-18Co cells promote the expression of Snail and ZEB1 of colon epithelial HCoEpiC cells through activation of TGF-β/Smad and HDAC1/2 up-regulation, resulting in EMT. TSA inhibits the EMT through repression of HDAC1/2/4 and TGF-β/Smads signalling and promotes apoptosis through activation of p38 MAPK (Green arrows represent promotion or activation of functions of CCD-18Co, blue arrows represent down-regulation of E-cadherin or up-regulation of vimentin and α-SMA, red lines represent inhibition of functions of TSA, and yellow arrows represent promotion or activation of TSA). (For interpretation of the references to colour in this figure legend, the reader is referred to the web version of this article).

involved in the TSA-induced apoptosis. To verify this hypothesis, VX-702, an inhibitor of p38 MAPK, was used. We found that the pre-treatment of VX-702 significantly reduced the TSA-induced apoptosis rates, with down-regulation of Bax and up-regulation of Bcl-2. These results suggest that regulation of p38 MAPK might play an important role in TAS-induced apoptosis.

5.6. Summary and prospect

Consistent with the chronology of the major events in the field of TSA/SB and colon cancer, our study for the first time suggest that TSA robustly inhibits the CCD-18Co-induced EMT and migration, and promotes the apoptosis in colon epithelial HCoEpiC cells, which are associated with its suppression of HDAC1/2. Although TSA inhibits the expression of HDAC4, its level dose not involve in the process of CCD-18Co-induced EMT. However, no effect of SB on the CCD-18Co-induced EMT is observed, which is inconsistent with that of previous studies. It shows that some difference exists between the effect of SB on cancer cells and TAF-induced epithelial cells, which may be in relation to cell type. The mechanisms underlying EMT inhibition by TSA include the suppression of TGF-β/Smad pathway and the activation of phosphorylated-p38 MAPK (Fig. 8). Our original study offers a new insight into the TAF-induced EMT in colon epithelium at an epigenetic level. As an epigenetic regulators, TSA can inhibit TAF-induced EMT and promote apoptosis, which may exert therapeutic affect in the prevention and treatment of carcinogenesis through targeting epithelial cells but not cancer cells. However, more *in vitro* and *in vivo* researches are needed to confirm the anti-cancer effect of TSA and the role of HDAC1/2 in carcinogenesis.

Funding

This work was supported by Natural Science Foundation of Guangdong Province (2018A030310060), China Postdoctoral Science Foundation (2018M643353).

Ethical approval

This article does not contain any studies with human participants or animals performed by any of the authors.

Informed consent

For this type of study, formal consent is not required.

Appendix A. Supplementary data

Supplementary material related to this article can be found, in the online version, at doi:https://doi.org/10.1016/j.biocel.2019.105565.

References

Adcock, I.M., 2007. HDAC inhibitors as anti-inflammatory agents. Br. J. Pharmacol. 150, 829–831.
Al Emam, A., Arbon, D., Jeeves, M., Kysela, B., 2018. Ku70 N-terminal lysines acetylation/deacetylation is required for radiation-induced DNA-double strand breaks repair. Neoplasma 65 (5), 708–719.
Aoto, K., Ito, K.l, Aoki, S., 2018. Complex formation between platelet-derived growth factor receptor β and transforming growth factor β receptor regulates the differentiation of mesenchymal stem cells into cancer-associated fibroblasts. Oncotarget 9 (75), 34090–34102.
Archer, S.Y., Johnson, J., Kim, H.J., Ma, Q., Mou, H., Daesety, V., Meng, S., Hodin, R.A., 2005. The histone deacetylase inhibitor butyrate downregulates cyclin B1 gene expression via a p21/WAF-1-dependent mechanism in human colon cancer cells. Am. J. Physiol. Gastrointest. Liver Physiol. 289 (4), G696–703.
Backlund, M.G., Mann, J.R., Holla, V.R., Shi, Q., Daikoku, T., Dey, S.K., DuBois, R.N., 2008. Repression of 15-hydroxyprostaglandin dehydrogenase involves histone deacetylase 2 and snail in colorectal cancer. Cancer Res. 68 (22), 9331–9337.
Barrasa, J.I., Olmo, N., Santiago-Gómez, A., Lecona, E., Anglard, P., Turnay, J., Lizarbe, M.A., 2012. Histone deacetylase inhibitors upregulate MMP11 gene expression through Sp1/Smad complexes in human colon adenocarcinoma cells. Biochim. Biophys. Acta 1823 (2), 570–581.
Bijelic, A., Aureliano, M., Rompel, A., 2019. Polyoxometalates as potential next-generation metallodrugs in the combat against Cancer. Angew. Chem. Int. Ed. Engl. 58 (10), 2980–2999.
Bordonaro, M., Lazarova, D.L., 2015. CREB-binding protein, p300, butyrate, and Wnt signaling in colorectal cancer. World J. Gastroenterol. 21 (27), 8238–8248.
Bordonaro, M., Lazarova, D.L., 2016. Determination of the role of CBP- and p300-Mediated wnt signaling on colonic cells. JMIR Res. Protoc. 5 (2), e66.
Bordonaro, M., Mariadason, J.M., Aslam, F., Heerdt, B.G., Augenlicht, L.H., 1999. Butyrate-induced apoptotic cascade in colonic carcinoma cells: modulation of the beta-catenin-Tcf pathway and concordance with effects of sulindac and trichostatin A but not curcumin. Cell Growth Differ. 10 (10), 713–720.
Bordonaro, M., Lazarova, D.L., Augenlicht, L.H., Sartorelli, A.C., 2002. Cell type- and promoter-dependent modulation of the Wnt signaling pathway by sodium butyrate. Int. J. Cancer 97 (1), 42–51.
Calonghi, N., Pagnotta, E., Parolin, C., Tognoli, C., Boga, C., Masotti, L., 2006. 9-Hydroxystearic acid interferes with EGF signalling in a human colon adenocarcinoma. Biochem. Biophys. Res. Commun. 342 (2), 585–588.
Catalano, M., D'Alessandro, G., Lepore, F., Corazzari, M., Caldarola, S., Valacca, C., et al.,

2015. Autophagy induction impairs migration and invasion by reversing EMT in glioblastoma cells. Mol. Oncol. 9 (8), 1612–1625.
Chen, X.F., Zhang, H.J., Wang, H.B., Zhu, J., Zhou, W.Y., Zhang, H., et al., 2012. Transforming growth factor-beta1 induces epithelial-to-mesenchymal transition in human lung cancer cells via PI3K/Akt and MEK/Erk1/2 signaling pathways. Mol. Biol. Rep. 39, 3549–3556.
Chen, X., Xiao, W., Chen, W., Luo, L., Ye, S., Liu, Y., 2013. The epigenetic modifier trichostatin A, a histone deacetylase inhibitor, suppresses proliferation and epithelial-mesenchymal transition of lens epithelial cells. Cell Death Dis. 4, e884. https://doi.org/10.1038/cddis.2013.416.
Chen, Q., Liu, G., Liu, S., Su, H., Wang, Y., Li, J., Luo, C., 2018. Remodeling the tumor microenvironment with emerging nanotherapeutics. Trends Pharmacol. Sci. 39 (1), 59–74.
Chen, B., Zhou, S., Zhan, Y., Ke, J., Wang, K., Liang, Q., et al., 2019. Dioscin Inhibits the Invasion and Migration of Hepatocellular Carcinoma HepG2 Cells by Reversing TGF-β1-Induced Epithelial-Mesenchymal Transition. Molecules 24 (12), E2222 pii:.
Choi, S.Y., Kee, H.J., Kurz, T., Hansen, F.K., Ryu, Y., Kim, G.R., et al., 2016. Class I HDACs specifically regulate E-cadherin expression in human renal epithelial cells. J. Cell. Mol. Med. 20 (12), 2289–2298. https://doi.org/10.1111/jcmm.12919.
Chowdhury, S., Ammanamanchi, S., Howell, G.M., 2009. Epigenetic targeting of transforming growth factor β receptor II and implications for Cancer therapy. Mol. Cell. Pharmacol. 1 (1), 57–70.
Dasgupta, N., Thakur, B.K., Ta, A., Dutta, P., Das, S., 2017. Suppression of spleen tyrosine kinase (Syk) by histone deacetylation promotes, whereas BAY61-3606, a synthetic syk inhibitor abrogates colonocyte apoptosis by ERK activation. J. Cell. Biochem. 118 (1), 191–203.
Dong, F., Liu, T., Jin, H., Wang, W., 2018. Chimaphilin inhibits human osteosarcoma cell invasion and metastasis through suppressing the TGF-β1-induced epithelial-to-mesenchymal transition markers via PI-3K/Akt, ERK1/2, and Smad signaling pathways. Can. J. Physiol. Pharmacol. 96 (1), 1–7.
Giménez-Bastida, J.A., Surma, M., Zieliński, H., 2015. In vitro evaluation of the cytotoxicity and modulation of mechanisms associated with inflammation induced by perfluorooctanesulfonate and perfluorooctanoic acid in human colon myofibroblasts CCD-18Co. Toxicol. In Vitro 29 (7), 1683–1691.
Giménez-Bastida, J.A., Laparra-Llopis, J.M., Baczek, N., Zielinski, H., 2018. Buckwheat and buckwheat enriched products exert an anti-inflammatory effect on the myofibroblasts of colon CCD-18Co. Food Funct. 9 (6), 3387–3397.
Glentis, A., Oertle, P., Mariani, P., Chikina, A., El Marjou, F., Attieh, Y., et al., 2017. Cancer-associated fibroblasts induce metalloprotease-independent cancer cell invasion of the basement membrane. Nat. Commun. 8 (1), 924.
Goulet, C.R., Champagne, A., Bernard, G., Vandal, D., Chabaud, S., Pouliot, F., et al., 2019. Cancer-associated fibroblasts induce epithelial-mesenchymal transition of bladder cancer cells through paracrine IL-6 signalling. BMC Cancer 19 (1), 137.
Hassig, C.A., Tong, J.K., Schreiber, S.L., 1997. Fiber-derived butyrate and the prevention of colon cancer. Chem. Biol. 4 (11), 783–789.
Hatakeyama, D., Ohmi, N., Saitoh, A., Makiyama, K., Morioka, M., Okazaki, H., et al., 2018. Acetylation of lysine residues in the recombinant nucleoprotein and VP40 matrix protein of Zaire Ebolavirus by eukaryotic histone acetyltransferases. Biochem. Biophys. Res. Commun. 504 (4), 635–640.
Hsu, Y.F., Sheu, J.R., Lin, C.H., Yang, D.S., Hsiao, G., Ou, G., Chiu, P.T., Huang, Y.H., Kuo, W.H., Hsu, M.J., 2012a. Trichostatin A and sirtinol suppressed survivin expression through AMPK and p38MAPK in HT29 colon cancer cells. Biochim. Biophys. Acta 1820 (2), 104–115.
Hsu, Y.F., Sheu, J.R., Lin, C.H., Yang, D.S., Hsiao, G., Ou, G., et al., 2012b. Trichostatin A and sirtinol suppressed survivin expression through AMPK and p38MAPK in HT29 colon cancer cells. Biochim. Biophys. Acta 1820 (2), 104–115.
Hsu, H.H., Wu, S.Y., Tang, S.E., Wu, G.C., Li, M.H., Huang, K.L., et al., 2015. Protection against reperfusion lung injury via aborgating multiple signaling cascades by trichostatin A. Int. Immunopharmacol. 25 (2), 267–275.
Ioannou, M., Kouvaras, E., Papamichali, R., Samara, M., Chiotoglou, I., Koukoulis, G., 2018. Smad4 and epithelial-mesenchymal transition proteins in colorectal carcinoma: an immunohistochemical study. J. Mol. Histol. 49 (3), 235–244.
Ji, M., Lee, E.J., Kim, K.B., Kim, Y., Sung, R., Lee, S.J., Kim, D.S., Park, S.M., 2015. HDAC inhibitors induce epithelial-mesenchymal transition in colon carcinoma cells. Oncol. Rep. 33 (5), 2299–2308.
Kelly, R.D.W., Chandru, A., Watson, P.J., Song, Y., Blades, M., Robertson, N.S., et al., 2018. Histone deacetylase (HDAC) 1 and 2 complexes regulate both histone acetylation and crotonylation in vivo. Sci. Rep. 8 (1), 14690.
Kim, Y.H., Lim, J.H., Lee, T.J., Park, J.W., Kwon, T.K., 2007. Expression of cyclin D3 through Sp1 sites by histone deacetylase inhibitors is mediated with protein kinase C-delta (PKC-delta) signal pathway. J. Cell. Biochem. 101 (4), 987–995.
Klampfer, L., Huang, J., Swaby, L.A., Augenlicht, L., 2004. Requirement of histone deacetylase activity for signaling by STAT1. J. Biol. Chem. 279 (29), 30358–30368.
Koledova, Z., 2017. 3D cell culture: an introduction. Methods Mol. Biol. 1612, 1–11.
Lakins, M.A., Ghorani, E., Munir, H., Martins, C.P., Shields, J.D., 2018. Cancer-associated fibroblasts induce antigen-specific deletion of CD8 + T Cells to protect tumour cells. Nat. Commun. 9 (1), 948.
Lamouille, S., Xu, J., Derynck, R., 2014. Molecular mechanisms of epithelial-mesenchymal transition. Nat. Rev. Mol. Cell Biol. 15 (3), 178–196.
Lazarova, D.L., Bordonaro, M., 2016. Vimentin, colon cancer progression and resistance to butyrate and other HDACis. J. Cell. Mol. Med. 20 (6), 989–993.
Lecona, E., Barrasa, J.I., Olmo, N., Llorente, B., Turnay, J., Lizarbe, M.A., 2008. Upregulation of annexin A1 expression by butyrate in human colon adenocarcinoma cells: role of p53, NF-Y, and p38 mitogen-activated protein kinase. Mol. Cell. Biol. 28 (15), 4665–4674.
Lee, H.S., Lin, Z., Chae, S., Yoo, Y.S., Kim, B.G., Lee, Y., et al., 2018. The chromatin remodeler RSF1 controls centromeric histone modifications to coordinate chromosome segregation. Nat. Commun. 9 (1), 3848.
Lei, W., Zhang, K., Pan, X., Hu, Y., Wang, D., Yuan, X., et al., 2010. Histone deacetylase 1 is required for transforming growth factor-beta1-induced epithelial-mesenchymal transition. Int. J. Biochem. Cell Biol. 42 (9), 1489–1497. https://doi.org/10.1016/j.biocel.2010.05.006.
Li, Q., Chen, H., 2012. Silencing of Wnt5a during colon cancer metastasis involves histone modifications. Epigenetics 7 (6), 551–558.
Li, X.l, Yoshida, M., Beppu, T., Lotan, R., 1996. Modulation of growth and differentiation of human colon carcinoma cells by histone deacetylase inhibitory trichostatins. Int. J. Oncol. 8 (3), 431–437.
Liu, D., Zhu, H., Gong, L., Pu, S., Wu, Y., Zhang, W., Huang, G., 2018. Histone deacetylases promote ER stress induced epithelial mesenchymal transition in human lung epithelial cells. Cell. Physiol. Biochem. 46 (5), 1821–1834.
Lobjois, V., Frongia, C., Jozan, S., Truchet, I., Valette, A., 2009. Cell cycle and apoptotic effects of SAHA are regulated by the cellular microenvironment in HCT116 multicellular tumour spheroids. Eur. J. Cancer 45 (13), 2402–2411.
Lyu, G., Guan, Y., Zhang, C., Zong, L., Sun, L., Huang, X., et al., 2018. TGF-β signaling alters H4K20me3 status via miR-29 and contributes to cellular senescence and cardiac aging. Nat. Commun. 9 (1), 2560.
Mali, A.V., Joshi, A.A., Hegde, M.V., Kadam, S.S., 2018. Enterolactone modulates the ERK/NF-κB/Snail signaling pathway in triple-negative breast cancer cell line MDA-MB-231 to revert the TGF-β-induced epithelial-mesenchymal transition. Cancer Biol. Med. 15 (2), 137–156.
Mobley, R.J., Abell, A.N., 2017. Controlling epithelial to mesenchymal transition through acetylation of histone H2BK5. J. Nat. Sci. 3 (9), e432 pii:.
Mrkvicova, A., Chmelarova, M., Peterova, E., Havelek, R., Baranova, I., Kazimirova, P., et al., 2019. The effect of sodium butyrate and cisplatin on expression of EMT markers. PLoS One 14 (1), e0210889.
Mukaida, N., Sasaki, S., 2016. Fibroblasts, an inconspicuous but essential player in colon cancer development and progression. World J. Gastroenterol. 22 (23), 5301–5316.
Musavi Shenas, M.H., Eghbal-Fard, S., Mehrisofiani, V., Abd Yazdani, N., Rahbar Farzam, O., Marofi, F., et al., 2018. MicroRNAs and signaling networks involved in epithelial-mesenchymal transition. J. Cell. Physiol. 2018 (November (11)). https://doi.org/10.1002/jcp.27489.
Nagarajan, D., Wang, L., Zhao, W., Han, X., 2017. Trichostatin A inhibits radiation-induced epithelial-to-mesenchymal transition in the alveolar epithelial cells. Oncotarget 8 (60), 101745–101759. https://doi.org/10.18632/oncotarget.21664.
Nakamura, M., Chiba, T., Kanayama, K., Kanzaki, H., Saito, T., Kusakabe, Y., et al., 2018. Epigenetic dysregulation in hepatocellular carcinoma; an up-to-date review. Hepatol Res Sep 20. https://doi.org/10.1111/hepr.13250.
Nawrocki, S.T., Carew, J.S., Douglas, L., Cleveland, J.L., Humphreys, R., Houghton, J.A., 2007. Histone deacetylase inhibitors enhance lexatumumab-induced apoptosis via a p21Cip1-dependent decrease in survivin levels. Cancer Res. 67 (14), 6987–6994.
Noh, H., Oh, E.Y., Seo, J.Y., Yu, M.R., Kim, Y.O., Ha, H., et al., 2009. Histone deacetylase-2 is a key regulator of diabetes- and transforming growth factor-beta1-induced renal injury. Am. J. Physiol. Renal Physiol. 297 (3), F729–39. https://doi.org/10.1152/ajprenal.00086.2009.
Orenay-Boyacioglu, S., Kasap, E., Gerceker, E., Yuceyar, H., Demirci, U., Bilgic, F., Korkmaz, M., 2018. Expression profiles of histone modification genes in gastric cancer progression. Mol. Biol. Rep. 2018 (September (24)). https://doi.org/10.1007/s11033-018-4389-z.
Papageorgis, P., 2015. TGFβ signaling in tumor initiation, epithelial-to-Mesenchymal transition, and metastasis. J. Oncol. 2015, 587193.
Park, I.H., Kang, J.H., Shin, J.M., Lee, H.M., 2016a. Trichostatin a inhibits epithelial mesenchymal transition induced by TGF-β1 in airway epithelium. PLoS One 11 (8), e0162058.
Park, I.H., Kang, J.H., Shin, J.M., Lee, H.M., 2016b. Trichostatin a inhibits epithelial mesenchymal transition induced by TGF-β1 in airway epithelium. PLoS One 11 (8), e0162058.
Pereira, C., Araújo, F., Barrias, C.C., Granja, P.L., Sarmento, B., 2015. Dissecting stromal-epithelial interactions in a 3D in vitro cellularized intestinal model for permeability studies. Biomaterials 56, 36–45.
Rajendran, P., Kidane, A.I., Yu, T.W., Dashwood, W.M., Bisson, W.H., Löhr, C.V., Ho, E., Williams, D.E., Dashwood, R.H., 2013. HDAC turnover, CtIP acetylation and dysregulated DNA damage signaling in colon cancer cells treated with sulforaphane and related dietary isothiocyanates. Epigenetics 8 (6), 612–623.
Raynal, N.J., Lee, J.T., Wang, Y., Beaudry, A., Madireddi, P., Garriga, J., et al., 2016. Targeting calcium signaling induces epigenetic reactivation of tumor suppressor genes in Cancer. Cancer Res. 76 (6), 1494–1505.
Rodríguez-Blanco, L.A., Rivera-Olvera, A., Escobar, M.L., 2019. Consolidation of an aversive taste memory requires two rounds of transcriptional and epigenetic regulation in the insular cortex. Behav. Brain Res. 356, 371–374.
Rusu, M.C., Pop, F., Hostiuc, S., Manta, L., Măru, N., Grigoriu, M., 2018. Transdifferentiations and heterogeneity in the stromal niches of uterine leiomyomas. Rom. J. Morphol. Embryol. 59 (3), 663–672.
Sanaei, M., Kavoosi, F., Roustazadeh, A., Shahsavani, H., 2018. In vitro effect of the histone deacetylase inhibitor valproic acid on viability and apoptosis of the PLC/PRF5 human hepatocellular carcinoma cell line. Asian Pac. J. Cancer Prev. 19 (9), 2507–2510.
Schäfer, C., Göder, A., Beyer, M., Kiweler, N., Mahendrarajah, N., Rauch, A., et al., 2017. Class I histone deacetylases regulate p53/NF-κB crosstalk in cancer cells. Cell. Signal. 29, 218–225.
Serpa, J., Caiado, F., Carvalho, T., Torre, C., Gon?alves, L.G., Casalou, C., Lamosa, P., Rodrigues, M., Zhu, Z., Lam, E.W., Dias, S., 2010. Butyrate-rich colonic microenvironment is a relevant selection factor for metabolically adapted tumor cells. J.

Biol. Chem. 285 (50), 39211–39223.
Servais, C., Erez, N., 2013. From sentinel cells to inflammatory culprits: cancer-associated fibroblasts in tumour-related inflammation. J. Pathol. 229, 198–207.
Shanmugam, M.K., Arfuso, F., Arumugam, S., Chinnathambi, A., Jinsong, B., Warrier, S., et al., 2017. Role of novel histone modifications in cancer. Oncotarget 9 (13), 11414–11426.
Shin, J., Carr, A., Corner, G.A., T?gel, L., Dávalos-Salas, M., Tran, H., et al., 2014. The intestinal epithelial cell differentiation marker intestinal alkaline phosphatase (ALPi) is selectively induced by histone deacetylase inhibitors (HDACi) in colon cancer cells in a Kruppel-like factor 5 (KLF5)-dependent manner. J. Biol. Chem. 289 (36), 25306–25316.
Siemens, H., Jackstadt, R., Hünten, S., Kaller, M., Menssen, A., Götz, U., et al., 2011. miR-34 and SNAIL form a double-negative feedback loop to regulate epithelial-mesenchymal transitions. Cell Cycle 10, 4256–4271.
Sikandar, S., Dizon, D., Shen, X., Li, Z., Besterman, J., Lipkin, S.M., 2010. The class I HDAC inhibitor MGCD0103 induces cell cycle arrest and apoptosis in colon cancer initiating cells by upregulating Dickkopf-1 and non-canonical Wnt signaling. Oncotarget 1 (7), 596–605.
Stempelj, M., Kedinger, M., Augenlicht, L., Klampfer, L., 2007. Essential role of the JAK/STAT1 signaling pathway in the expression of inducible nitric-oxide synthase in intestinal epithelial cells and its regulation by butyrate. J. Biol. Chem. 282 (13), 9797–9804.
Sun, L., Fang, J., 2016. Epigenetic regulation of epithelial-mesenchymal transition. Cell. Mol. Life Sci. 73 (23), 4493–4515.
Sundararajan, V., Tan, M., Tan, T.Z., Ye, J., Thiery, J.P., Huang, R.Y., 2019. SNAI1 recruits HDAC1 to suppress SNAI2 transcription during epithelial to mesenchymal transition. Sci. Rep. 9 (1), 8295.
Tang, F.Y., Pai, M.H., Chiang, E.P., 2012. Consumption of high-fat diet induces tumor progression and epithelial-mesenchymal transition of colorectal cancer in a mouse xenograft model. J. Nutr. Biochem. 23 (10), 1302–1313.
Tang, J., Yan, H., Zhuang, S., 2013. Histone deacetylases as targets for treatment of multiple diseases. Clin. Sci. 124, 651–662.
Ulrich, S., Wächtershäuser, A., Loitsch, S., von Knethen, A., Brüne, B., Stein, J., 2005. Activation of PPARgamma is not involved in butyrate-induced epithelial cell differentiation. Exp. Cell Res. 310 (1), 196–204.
von Burstin, J., Eser, S., Paul, M.C., Seidler, B., Brandl, M., Messer, M., et al., 2009. E-cadherin regulates metastasis of pancreatic cancer in vivo and is suppressed by a SNAIL/HDAC1/HDAC2 repressor complex. Gastroenterology 137 (1), 361–371. https://doi.org/10.1053/j.gastro.2009.04.004. 371.e1-5.
Wade, P.A., 2001. Transcriptional control at regulatory checkpoints by histone deacetylases: molecular connections between cancer and chromatin. Hum. Mol. Genet. 10, 693–698.
Wang, H.G., Huang, X.D., Shen, P., Li, L.R., Xue, H.T., Ji, G.Z., 2013a. Anticancer effects of sodium butyrate on hepatocellular carcinoma cells in vitro. Int. J. Mol. Med. 31 (4), 967–974.
Wang, H.G., Huang, X.D., Shen, P., Li, L.R., Xue, H.T., Ji, G.Z., 2013b. Anticancer effects of sodium butyrate on hepatocellular carcinoma cells in vitro. Int. J. Mol. Med. 31 (4), 967–974. https://doi.org/10.3892/ijmm.2013.1285.
Wang, X., Zhang, W., Sun, X., Lin, Y., Chen, W., 2018a. Cancer-associated fibroblasts induce epithelial- mesenchymal transition through secreted cytokines in endometrial cancer cells. Oncol. Lett. 15 (4), 5694–5702.
Wang, Z.F., Ma, D.G., Wang, L., Feng, L., Fu, J.W., Li, Y., et al., 2018b. Paeoniflorin inhibits migration- and invasion-promoting capacities of gastric Cancer Associated fibroblasts. Chin. J. Integr. Med. 2018 (October (25)). https://doi.org/10.1007/s11655-018-2985-3.
Wang, L., Li, X., Ren, Y., Geng, H., Zhang, Q., Cao, L., et al., 2019. Cancer-associated fibroblasts contribute to cisplatin resistance via modulating ANXA3 in lung cancer cells. Cancer Sci. 2019 (March (13)). https://doi.org/10.1111/cas.13998.
Wawro, M.E., Chojnacka, K., Wieczorek-Szukała, K., Sobierajska, K., Niewiarowska, J., 2018. Invasive Colon Cancer cells induce transdifferentiation of endothelium to cancer-associated fibroblasts through microtubules enriched in Tubulin-β3. Int. J. Mol. Sci. 20 (1), E53 pii:.
Wei, J., Li, Z., Yuan, F., 2014. Evodiamine might inhibit TGF-beta1-induced epithelial-mesenchymal transition in NRK52E cells via Smad and PPAR-gamma pathway. Cell Biol. Int. 38 (7), 875–880.
Xiao, W., Chen, X., Liu, X., Luo, L., Ye, S., Liu, Y., 2014. Trichostatin A, a histone deacetylase inhibitor, suppresses proliferation and epithelial-mesenchymal transition in retinal pigment epithelium cells. J. Cell. Mol. Med. 18 (4), 646–655. https://doi.org/10.1111/jcmm.12212.
Xie, L., Santhoshkumar, P., Reneker, L.W., Sharma, K.K., 2014. Histone deacetylase inhibitors trichostatin A and vorinostat inhibit TGFβ2-induced lens epithelial-to-mesenchymal cell transition. Invest. Ophthalmol. Vis. Sci. 55 (8), 4731–4740. https://doi.org/10.1167/iovs.14-14109.
Xu, L., Liu, N., Gu, H., Wang, H., Shi, Y., Ma, X., et al., 2017. Histone deacetylase 6 inhibition counteracts the epithelial-mesenchymal transition of peritoneal mesothelial cells and prevents peritoneal fibrosis. Oncotarget 8 (51), 88730–88750.
Yang, W., Gong, X., Wang, X., Huang, C., 2018. A mediator of phosphorylated Smad2/3, evodiamine, in the reversion of TAF-induced EMT in normal colonic epithelial cells. Invest. New Drugs 2018 (November (29)). https://doi.org/10.1007/s10637-018-0702-x.
Yao, K., Ye, P.P., Tan, J., Tang, X.J., Shen Tu, X.C., 2008. Involvement of PI3K/Akt pathway in TGF-beta2-mediated epithelial mesenchymal transition in human lens epithelial cells. Ophthalmic Res. 40, 69–76.
Yin, L., Laevsky, G., Giardina, C., 2001. Butyrate suppression of colonocyte NF-kappa B activation and cellular proteasome activity. J. Biol. Chem. 276 (48), 44641–44646.
Yoshikawa, M., Hishikawa, K., Marumo, T., Fujita, T., 2007a. Inhibition of histone deacetylase activity suppresses epithelial-to-mesenchymal transition induced by TGF-beta1 in human renal epithelial cells. J. Am. Soc. Nephrol. 18, 58–65.
Yoshikawa, M., Hishikawa, K., Marumo, T., Fujita, T., 2007b. Inhibition of histone deacetylase activity suppresses epithelial-to-mesenchymal transition induced by TGF-beta1 in human renal epithelial cells. J. Am. Soc. Nephrol. 18 (1), 58–65.
Yoshikawa, M., Hishikawa, K., Marumo, T., Fujita, T., 2007c. Inhibition of histone deacetylase activity suppresses epithelial-to-mesenchymal transition induced by TGF-beta1 in human renal epithelial cells. J. Am. Soc. Nephrol. 18, 58–65.
Yu, X., Ma, R., Wu, Y., Zhai, Y., Li, S., 2018. Reciprocal regulation of metabolic reprogramming and epigenetic modifications in Cancer. Front. Genet. 9, 394.
Zhan, Y., Gong, K., Chen, C., Wang, H., Li, W., 2012. P38 MAP kinase functions as a switch in MS-275-induced reactive oxygen species-dependent autophagy and apoptosis in human colon cancer cells. Free Radic. Biol. Med. 53 (3), 532–543.
Zhang, L., Kang, W., Lu, X., Ma, S., Dong, L., Zou, B., 2018. Weighted gene co-expression network analysis and connectivity map identifies lovastatin as a treatment option of gastric cancer by inhibiting HDAC2. Gene 681, 15–25.
Zhu, X., Han, S., Wu, S., Bai, Y., Zhang, N., Wei, L., 2019. Dual role of twist1 in cancer-associated fibroblasts and tumor cells promoted epithelial-mesenchymal transition of esophageal cancer. Exp. Cell Res. 375 (2), 41–50.